

# ISTITUTO NAZIONALE DI FISICA NUCLEARE

Sezione di Milano

---

INFN/TC-98/35  
26 Novembre 1998

F. Alessandria, G. Ambrosio:

**ANALYTICAL STUDY OF THE BEHAVIOUR OF A COLD MASS SUPPORT  
DURING THE COOLDOWN AND THE ENERGIZATION OF THE ATLAS  
BARREL TOROID**

**PACS:** 07.20.Mc

*Published by SIS-Pubblicazioni  
Laboratori Nazionali di Frascati*



**ANALYTICAL STUDY OF THE BEHAVIOUR OF A COLD MASS SUPPORT  
DURING THE COOLDOWN AND THE ENERGIZATION OF THE ATLAS  
BARREL TOROID**

F. Alessandria, G. Ambrosio  
INFN–Sezione di Milano, Laboratorio LASA, Via Fratelli Cervi 201, I–20090 Segrate (Milano),  
Italy

**Abstract**

During the cooldown the cold mass supports are subjected to bending deformations because of the cold mass contraction. The supports have articulations at both ends in order to accommodate the displacements between the cold mass and the warm structure. The bending deformation of the supports will depend on the stick and slip behaviour of the sliding surfaces. In this report the behaviour of a support, subjected to a constant tensile load during the displacement of an end of its, has been studied. The displacement considered (45 mm) is the one foreseen for the outer supports (i.e. the most distant from the centre of each coil).

The behaviour of the support has also been studied during the magnet energization, taking into account the increment of the tensile force and the displacement of the support end, due to the coil elongation because of the magnetic forces. The aim of this part of the study is to check the possibility of a sliding of the articulations during the magnet energization.

At the end two studies of the warm pivot rotation are reported. In the first study the inertia energy and the dynamic friction are considered in order to check an assumption done in the analysis of the support dynamic during the cooldown. In the second study the change of the deformation energy and the work of the external forces are considered in order to check a rotation computed during the cooldown.

**Symbols used:**

$C_0$	moment at the junction between the flexible part and the warm rigid end,
$C$	moment at the junction between the flexible part and the cold rigid end,
$E$	Young modulus,
$F_R$	radial component of the reaction force,
$F_T$	tangential component of the reaction force due to the friction,
$H$	elastic deformation energy of the flexible part of the support,
$I$	inertia momentum of the warm rigid articulation respect to its rotation axis,
$J_1, J_2$	inertia momentum of the two flexible parts of the beam,
$L_a$	work done by the friction force,
$M$	bending moment $M=M(z)$ ,
$N$	component of the force normal to the support section in $z = 0$ ,
$P$	component of the force parallel to the support section in $z = 0$ ,
$R$	reaction,
$S, T$	lines in the centre of each antifriction strip of the cold articulation where the reaction forces are applied,
$X_p, X_c, Y_p, Y_c$	coefficients depending on the geometrical parameters and $N$ (see appendix A),
$h$	distance from the sliding surface of the warm end to the flexible part,
$k$	distance from the sliding surface of the cold end to the flexible part,
$l$	flexible beam length,
$l_1, l_2$	length of a part of the flexible beam with a constant cross section,
$r_{ca}$	cold articulation inner radius,
$r_{wa}$	warm articulation inner radius,
$s$	deflection of the cold end of the flexible part,
$x, y$	fixed co-ordinate. system centred in the warm articulation,
$z, \eta$	co-ordinate system centred in the warm end of the flexible part, the $z$ axis is tangential to the flexible part,
$\beta$	the angle between the radial plane crossing the line $S$ (or $T$ ) and the middle plane of the rigid end of the support (see Fig. 3),
$\varepsilon$	$\tan(\varepsilon) = P/N$ ,
$\phi$	angle between the reaction and its radial component in the warm end,
$\mu_d$	dynamic friction coefficient of the contact surface,
$\mu_{\min}$	value of the friction coefficient used to obtain the new equilibrium condition after a rotation,
$\mu_s$	static friction coefficient of the contact surface,
$\nu$	angle between the reaction and its radial component in each contact region of the cold end,
$\theta$	angular position of the cold end respect to the co-ordinate system $z, \eta$
$\psi$	angular position of the point where reaction forces are applied,
$\zeta$	angle of the $z$ axis respect to the $x$ axis,

## 1. - INTRODUCTION

In order to support the cold mass of the ATLAS Barrel Toroid (BT) the use of 8 supports for each coil is foreseen.

These supports are linked both to the warm structure and to the cold mass through articulated ends (Fig. 1).

The supports withstand the component of the cold mass weight parallel to their axis (compressive or tensile according to the coil orientation), and the magnetic forces (tensile in any coil).

During the cooldown the support end linked to the cold mass follows its thermal contraction. For the outer supports the contraction results in a 45 mm displacement.

The displacement occurs while the supports withstand the coil weight. In case of no friction the articulations are free to rotate and the axis of the support will always remain straight, under the only action of axial forces. Friction forces make the supports follow the contraction by means of their elastic deformation. When friction forces reach their limit in one articulation, then the articulation rotates and the support assumes a new shape less deformed than before.

Because of this behaviour the support may have an important bending deformation at the end of the cold mass contraction.

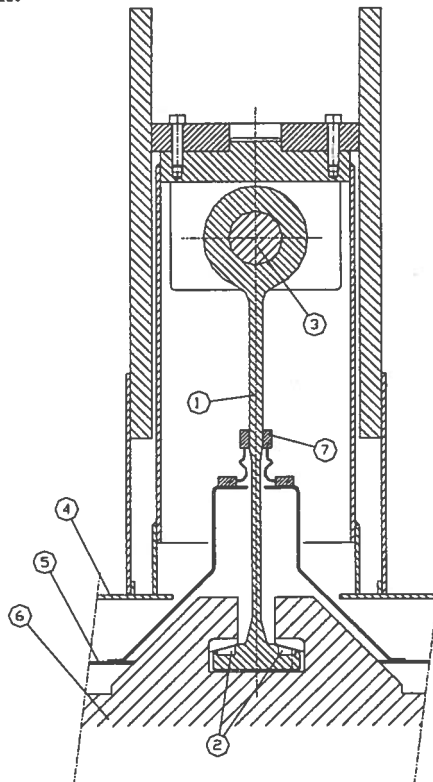


**Figure 1: The cold mass support, 1- support, 2- antifriction insert, 3- pivot with antifriction bushing, 4- vacuum chamber, 5- thermal shield, 6- coil casing, 7- thermal link.**

During the energization the magnetic forces change the shape of each coil incrementing its length. This deformation results in a new displacement of the ends of each support. In case of the outer supports it is about 3 mm (in the direction opposite to the previous deformation).

This movement comes with an increasing tensile load in the supports due to the magnetic forces. The value of these forces much higher than the weight should avoid any sliding in the articulations especially at the highest fields.

The bending deformation of the supports in this phase will add to the previous deformation. The aim of this part of the study is therefore to evaluate if excessive deformations could be reached and also if the lowering of the friction coefficient of the contact surface (Glicodur) due to the pressure increment [1] may cause a rotation at high fields.

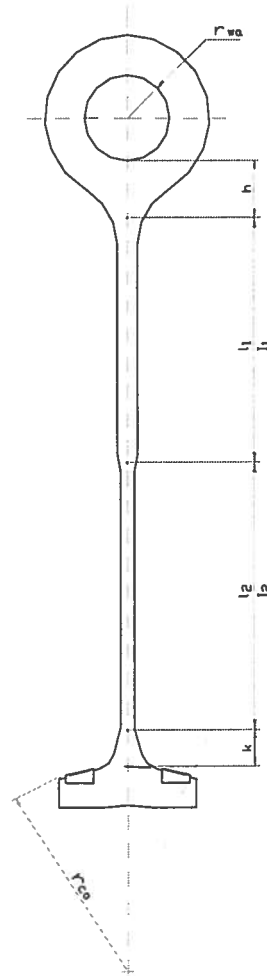


**Figure 2: Support cross section.**

## 2. - SUPPORT DESCRIPTION

In this report the support is supposed consisting of three parts (Fig. 2):

- a rigid end joined to the warm structure by means of an articulation with inner radius  $r_{wa}$  (warm articulation);
- a rigid end joined to the cold mass by means of an articulation with inner radius  $r_{ca}$  (cold articulation);

- a flexible beam of length  $l$ , divided in two parts with the following lengths and inertia moments:  $l_1, J_1$  and  $l_2, J_2$ . The flexible beam starts at a distance  $h$  from the sliding surface of the warm end, and terminates at a distance  $k$  from the sliding surface of the cold end.

The bending deformation of the flexible part is indicated by the displacement  $s$  and by the rotation  $\theta$  of its cold end in the reference system  $z, \eta$  according to the usual conventions for beams (Fig. 3). The reference system has the origin in the warm end of the flexible part and the  $z$  axis is oriented as the tangent to the flexible part in that point.

The position of the cold articulation is given using the reference system  $x, y$  whose origin is the centre of the warm articulation. This reference system remain fix during the cooldown and the energization.

Referring to Fig. 3 the position of the centre of the cold articulation is linked to the other parameters by the following relation:

$$y = (r_{wa} + h + l) \sin(\zeta) - \cos(\zeta)s + (r_{ca} + k) \sin(\zeta - \vartheta) \quad (1.)$$

where  $\zeta$  is the angle of the  $z$  axis respect to the  $x$  axis.

The same relation for the  $x$  axis is not interesting because only one support is studied and the cold mass is supposed to be free to move in vertical direction.

### 3. - FORCES AND STRAIN IN THE FLEXIBLE PART

The following study refers to a support of the four highest coils of the toroid because the support is supposed to be in tension during the cooldown.

The flexible part is subjected at both the ends to the forces applied by the rigid part of the support (see Fig. 3):

- the two forces  $N$  parallel to the  $z$  axis, with equal intensity and opposite direction,
- the two transversal forces  $P$ , with equal intensity and opposite direction,
- $C_0$ : the moment at the junction between the flexible part and the warm rigid end,
- $C$ : the moment at the junction between the flexible part and the cold rigid end.

In order to have equilibrium it should be:

$$C + C_0 = Pl - Ns \quad (2.)$$

The bending deformation of both the two flexible parts can be described by the following relation ( $E$  is the Young modulus):

$$\frac{d^2 \eta}{dz^2} - \frac{N}{EJ} \eta = \frac{C_0}{EJ} - \frac{P}{EJ} z \quad (3.)$$

where the contribution of the axial force  $N$  (acting because of the deformation) has been taken into account because it's not negligible.

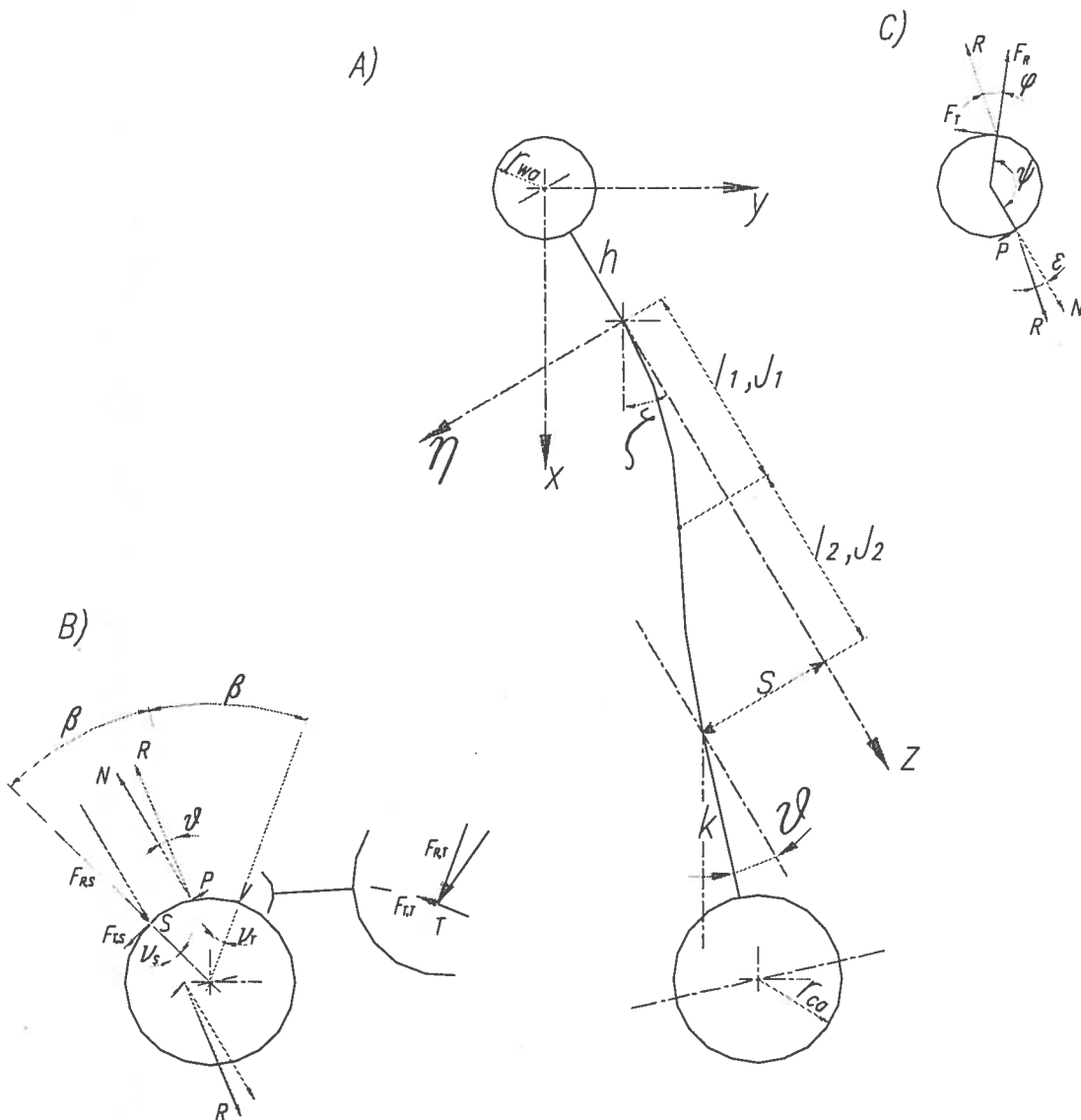


**Figure 3: The model of the support and the applied forces. A) Whole model, B) cold end, C) warm end.**

By integration and imposing the boundary conditions at the ends, the expressions of the deformation  $\eta(z)$  and of its derivative  $d\eta/dz$  can be obtained.

These expressions, evaluated in  $z=l$ , allow the calculus of the applied forces as function of the deflection ( $s$ ) and of the orientation of the cold end ( $\theta$ ).

It is:

$$\frac{P}{N} = X_p \frac{s}{l} + Y_p \vartheta \quad (4.)$$

$$\frac{C_0}{N} = X_c s + Y_c l \vartheta$$

where the coefficients  $X_p$ ,  $X_c$ ,  $Y_p$  and  $Y_c$  depend on the geometrical parameters of the flexible part and on the applied force  $N$ . Their expressions are reported in appendix A.



Therefore if the force  $N$  is a known constant, the force  $P$  and the momentum  $C_0$  can be evaluated as function of the deformation of the flexible part.

#### 4. - REACTIONS IN THE WARM ARTICULATION

The warm articulation is joint to the warm structure by means of a pivot fitting the circular hole having radius  $r_{wa}$ .

The equilibrium of the warm rigid end of the support impose the momentum ( $C_0$ ) and the forces ( $N, P$ ) applied by the flexible part in  $z = 0$  being equilibrated by the reactions applied from the pivot to the surface of the hole.

The reaction forces are supposed to be concentrated in a point instead of being applied on an arc as it is in reality. The validity of this approximation is shown in appendix B.

The reaction forces consist of a radial force ( $F_R$ ) and of a friction force ( $F_T$ ) that is tangential to the pivot surface and oriented in such a way to contrast the support rotation (Figure 3).

Applying the equilibrium equations at the interface between the warm rigid end and the flexible part, the radial force, the tangential force and their application point can be evaluated.

Referring to Fig. 3 the angle  $\psi$  indicating the application point of the reaction force is given by:

$$\sin(\varepsilon) + \frac{C_0 + Ph}{r_{wa}N} \cos(\varepsilon) = \sin(\psi + \varepsilon) \quad (5.)$$

where

$$\tan(\varepsilon) = \frac{P}{N}. \quad (6.)$$

The angle  $\phi$  between the reaction and its radial component is given by:

$$\phi = \pi - \psi - \varepsilon \quad (7.)$$

The rigid end of the support, subjected to  $N, P$  and  $C_0$ , is in equilibrium until the following relation holds:

$$|\operatorname{tg}(\phi)| \leq \mu_s, \quad (8.)$$

where  $\mu_s$  is the static friction coefficient between the contact surfaces.

In case of a rigid end consisting of a pivot fitting an hole in the warm structure, the position of the application point is different but the sliding condition is the same.

## 5. - REACTIONS IN THE COLD MASS ARTICULATION

The cold end of the support lean against a cylindrical surface made of two pieces of the coil casing. The contact surface consists of two strips of low friction material acting in order to reduce the forces against the support rotation. The reaction forces are supposed to be applied on the line (S or T) in the centre of each strip (Fig. 3).

They balance the forces ( $N, P$ ) and the momentum ( $C$ ) transferred from the flexible part of the support to its cold rigid end.

The reaction forces in both the contact surfaces consist of a radial force and of a tangential friction force oriented in such a way to contrast the support rotation.

Applying the equilibrium equations at the interface between the cold rigid end and the flexible part, it's possible to evaluate the radial and tangential forces and their application points. In this study the ratio between the tangential and the radial forces is supposed to be the same in the two sliding regions. This is sure at the sliding limit.

The angle  $\nu$  between the reaction and its radial component in each contact region is given by:

$$\sin(2\nu - \varepsilon + \vartheta) = (2 \cos \beta - 1) \sin(\varepsilon - \vartheta) + 2 \frac{C + Pk - Nk\vartheta}{r_{ca} N} \cos(\varepsilon) \cos(\beta) \quad (9.)$$

where  $\beta$  is the angle between the radial plane crossing the line S (or T) and the middle plane of the rigid end of the support (see Fig. 3).

The cold end of the support, subjected to  $N, P$  and  $C$ , is in equilibrium until the following relation holds:

$$|\operatorname{tg}(\nu)| \leq \mu_s \quad (10.)$$

where  $\mu_s$  is the static friction coefficient between the contact surfaces.

## 6. - SUPPORT MOVEMENTS DURING COOLDOWN AND ENERGIZATION

Before starting the cooldown, the support is in equilibrium without any deflection and equation (1) is trivially satisfied.

The effect of the cooldown is imposed modifying the position of the cold end of the support ( $y$ ).

During the first part of the displacement the support bends without any rotation of the ends because of friction. Therefore the ends inclination doesn't change while the deflection ( $s$ ) changes continuously according to the  $y$  variation.

$$\begin{aligned} \zeta &= \zeta_{in} \\ \vartheta &= \vartheta_{in} \\ s &= \frac{(r_{wa} + h + l) \sin(\zeta_{in}) + (r_{ca} + k) \sin(\zeta_{in} - \vartheta_{in}) - y}{\cos(\zeta_{in})} \end{aligned} \quad (11.)$$

Using the previous formulas (4, 5 and 9) the force and the momentum at the ends of the flexible part, and the reaction force on the contact surfaces can be known.

The first rotation occurs in the first articulation where the sliding condition is reached. After the rotation the support assumes a new equilibrium condition. If the rotation occurs in the cold end, then  $y$  and  $\zeta$  remain constant during the rotation, while  $s$  and  $\theta$  change their value. If the rotation occurs in the warm articulation,  $y$  and  $\zeta - \theta$  remain constant while  $s$ ,  $\zeta$ , and  $\theta$  change their value. The change of  $\theta$  is due to the fact that the reference system  $z, \eta$  is located on the warm articulation.  $\zeta - \theta$  is the orientation of the cold articulation in a fixed reference system. Remaining it constant the warm articulation is free to rotate without generating a rotation of the cold articulation.

The new equilibrium condition after the rotation depends on the dynamic friction coefficient assumed. The angle  $\theta$  or  $\zeta$  is supposed to change until the sliding condition is reached using a value of the friction coefficient ( $\mu_{\min}$ ) lower than the dynamic friction coefficient.

In both the articulations a contact surface is made of a Teflon-based low friction material. The static and the dynamic friction coefficient ( $\mu_d$ ) are supposed not very different ( $\mu_d = 7/8 \mu_s$ ). For this reason also  $\mu_{\min}$  can be supposed not too different from the static friction coefficient, and the value  $\mu_{\min} = 3/4 \mu_s$  has been used (see sections 10 and 11 for details).

Restarting this analysis from the new equilibrium condition it's possible to find where the next rotation will occur. Repeating this stick (support bending) and slip (articulation rotation) procedure the behaviour of the support during all the cooldown can be studied.

The deformation of the support at the end of the cooldown will depend on the final value of  $\theta$  and of the deflection at the cold end ( $s$ ).

During the magnet energization three new features must be taken into account:

- The magnetic forces increase the value of  $N$ .
- They also cause an elongation of the coil casing generating a displacement of the cold end of the support in the direction opposite to the displacement caused by the cooldown. In this study the variations of  $N$  and  $y$  are supposed to be proportional.
- The friction coefficient decreases because of the increment of the pressure on the contact surfaces. This behaviour is deduced from the data showing a decrement of the sliding friction coefficient vs. pressure in [1].

The calculus procedure is the same as before, but  $N$  and  $\mu_s$  are now depending on  $y$ . The starting point is the configuration of the support at the end of the cooldown.

The aim of this analysis is to check the possibility of a rotation because it could produce a movement of the coil and a quench of the magnet. The increment of the force applied on the support ( $N$ ) acts against this possibility, but the lowering of the friction coefficient can generate it.

## 7. - COMPUTATION TECHNIQUE

The computation is done using Mathcad 5.0.

All the variables used are written as function of the variables  $y$ ,  $\theta$  and  $\zeta$ , and of the geometrical parameters.  $N$  is set as a parameter because its use as a variable would require a very long expression to define some of the other variables.

The values of  $y$  that solve equation (8) or (10) are searched by means of a numerical equation solver. The two solutions are compared to see what articulation will slide first.

If the rotation occurs in the cold articulation, the value of the angle after the rotation is searched solving numerically the following equation respect to  $\theta$ , while  $y$  and  $\zeta$  are fixed.

$$|tg(v(y, \theta, \zeta))| = \mu_{\min} \quad (12.)$$

If the rotation occurs in the warm articulation, the following equation is solved numerically respect to  $\zeta$  while  $y$  and  $\zeta - \theta$  are fixed.

$$|tg(\psi(y, \theta(\zeta), \zeta))| = \mu_{\min} \quad (13.)$$

Naming  $\zeta'$  the solution,  $\zeta_{in}$  and  $\theta_{in}$  the angles before the rotation, their values after the rotation are:

$$\begin{aligned} \zeta &= \zeta' \\ \vartheta &= \vartheta_{in} - (\zeta' - \zeta_{in}) \end{aligned} \quad (14.)$$

This procedure is repeated after each rotation up to the end of the cold articulation displacement:  $\Delta y = -45$  mm.

The behaviour of the support during the energization has been studied comparing the values of  $|tg(v)|$  and  $|tg(\psi)|$  with the values of  $\mu_s$  at the maximum field and at some fraction of it.

## 8. - RESULTS OF THE STUDY OF A SUPPORT

The results of the study of an outer support (i.e. the most distant from the centre of the coil) is here reported. The coil chosen is one of the highest (i.e. coil number 4 or 6 according to the Barrel Toroid numeration) having the supports always under a tensile force (only the weight during the cooldown, the weight and the magnetic forces during the energization).

Dimensions and parameters of the support together with its starting condition are reported in table 1.

Figures 4 and 5 show the results of the analysis during the cooldown.

In Fig. 4 the orientation of both the articulations is shown. On the abscissa there is the position of the centre of the cold articulation that is supposed to move from 22.5 to -22.5 mm. On the ordinate there is the orientation of the articulations:  $\zeta$  for the warm one,  $\zeta - \theta$  for the cold one. Every couple of marks with the same abscissa show the state of the two articulations after a rotation. The rotated articulation is the one whose orientation is different from the previous one.

	Symbol	value	dimens.
Length of the thicker part of the flexible beam,	$l_1$	387	mm
length of the thinner part of the flexible beam,	$l_2$	395	mm
distance from the warm sliding surface to flexible part,	$h$	58	mm
distance from the cold sliding surface to flexible part,	$k$	37	mm
warm articulation inner radius,	$r_{wa}$	62	mm
cold articulation inner radius,	$r_{ca}$	300	mm
inertia mom. of the thicker part of the flexible beam,	$J_1$	$5.4 \cdot 10^5$	N mm
inertia mom. of the thinner part of the flexible beam,	$J_2$	$1.6 \cdot 10^5$	N mm
component of the force parallel to the z axis	$N$	$6 \cdot 10^4$	N
horizontal position of the cold articulation	$y$	22.5	mm
warm articulation orientation	$\zeta$	1.04	deg.
Deflection of the cold end	$s$	0	mm
rotation of the cold art. respect to the warm one	$\theta$	0	deg
static friction coefficient	$\mu_s$	0.15	
coefficient used to find equilibrium after a rotation	$\mu_{min}$	0.1125	

**Table 1: Support parameters and starting condition.**

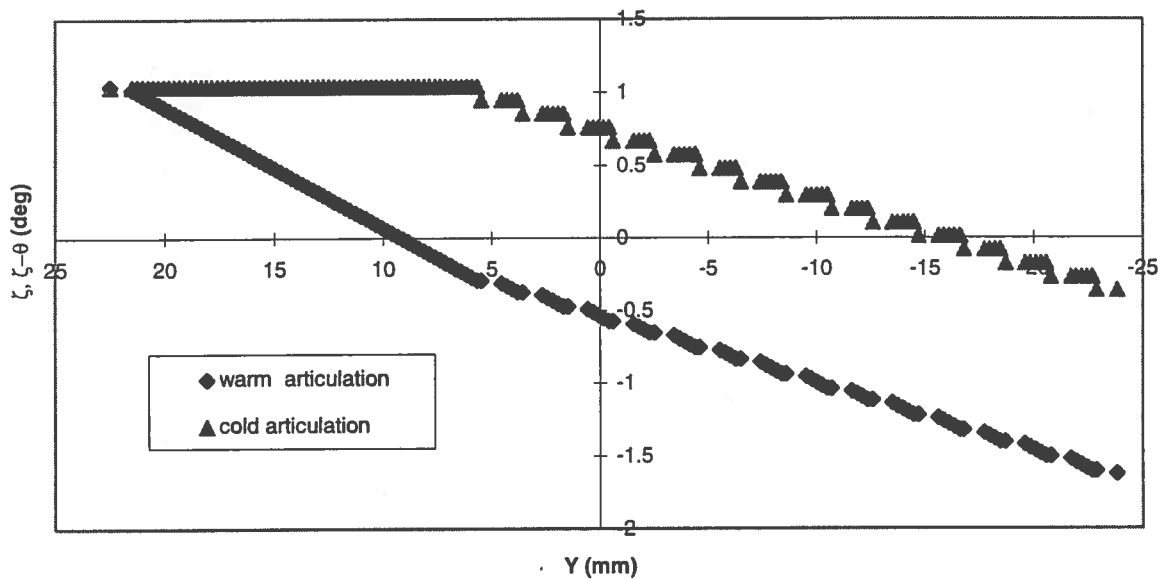


**Figure 4: Orientation of both the articulations during the cooldown.**

It can be noted that:

- during the first 17 mm of displacement only the warm articulation rotates, while during the remaining part of the path the two articulations alternate their rotations: three or four in the warm articulation after each rotation in the cold one;
- in the final position the cold articulation is less rotated than the warm one because its inertia is higher than that of the warm articulation.

- the difference between the articulations orientation ( $\theta$ ) increases until the first rotation of the cold articulation occurs, remaining almost constant during the following movements.

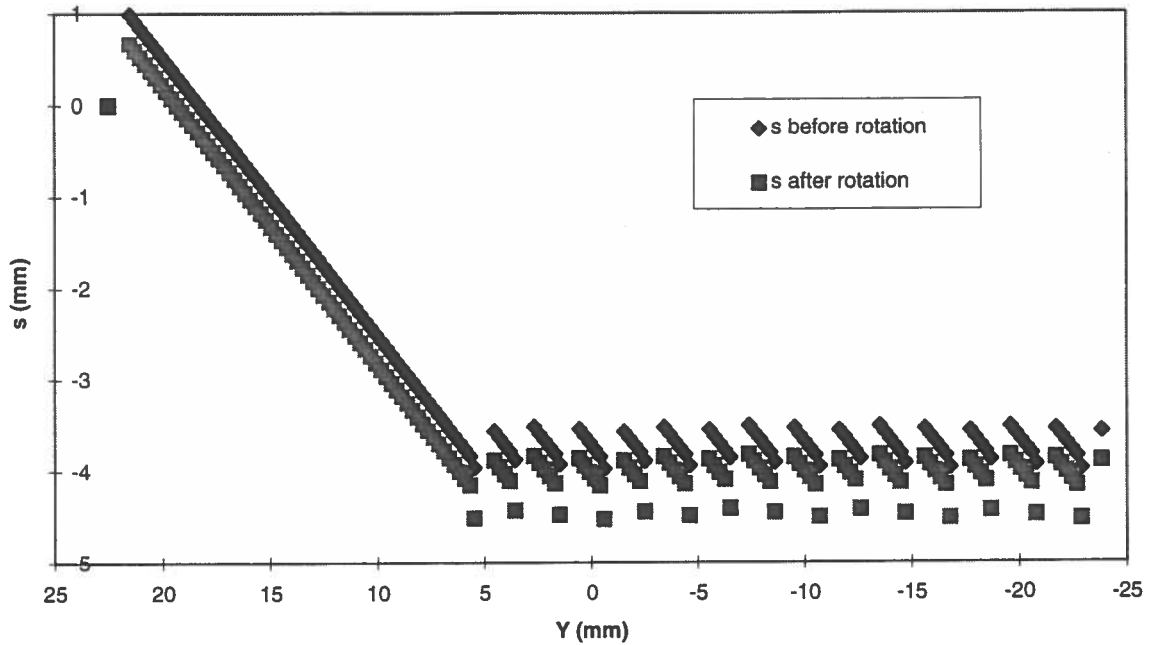


**Figure 5: Deflection at the cold end of the flexible part of the support during the cooldown. The values before and after each rotation are shown.**

In Fig. 5 the deflection of the cold end of the flexible part is reported. Both the values before and after each rotation are shown. The value of the deflection oscillates between the two lines during all the cooldown.

In Table 2 all data indicating the support deflection at the end of the cooldown are reported.

	symbol	value	dimens.
Horizontal position of the cold articulation	$y$	22.5	mm
warm articulation orientation	$\zeta$	-1.58	deg
deflection of the cold end	$s$	-4.09	mm
rotation of the cold art. respect to the warm one	$\theta$	-1.31	deg

**Table 2: Support condition after the cooldown.**

Figure 6 shows the results of the analysis during the magnet energization. The ratio between the tangential and the normal component of the pivot reaction is reported for both the articulations. Also reported is the static friction coefficient vs. load of the low friction material. The data shown have been extrapolated from those of the dynamic friction coefficient [1]. They are reported with positive and negative values to take into account the possibility of both clockwise and anticlockwise rotations.

Three studies have been done starting from different conditions:

- before the last rotation of the warm articulation,

- after the last rotation of the warm articulation,
- after the last rotation of the cold articulation.

The first two conditions are close to the final one of the previous analysis (i.e. behaviour during the cooldown), the third condition is the most pessimistic. It can be seen that the ratio  $F_{\text{tang}}/F_{\text{rad}}$  decreases during the energization in the cold pivot, while it changes its value and increases with the field in the warm pivot. The final values of this ratio in the warm pivot are shown in the following table for each starting condition.

The conclusion of this case is therefore that a Teflon filled compound allows acceptable deformations of the support during the cooldown but brings a high risk of rotations at high field.

Starting condition:	$F_{\text{tang}} / F_{\text{rad}}$ at maximum load
before the last rotation of the warm pivot	- 0.048
after the last rotation of the warm pivot	- 0.049
after the last rotation of the cold pivot	- 0.054

**Table 3: The final values of the ratio  $F_{\text{tang}} / F_{\text{rad}}$  in the warm pivot according to different starting conditions.**

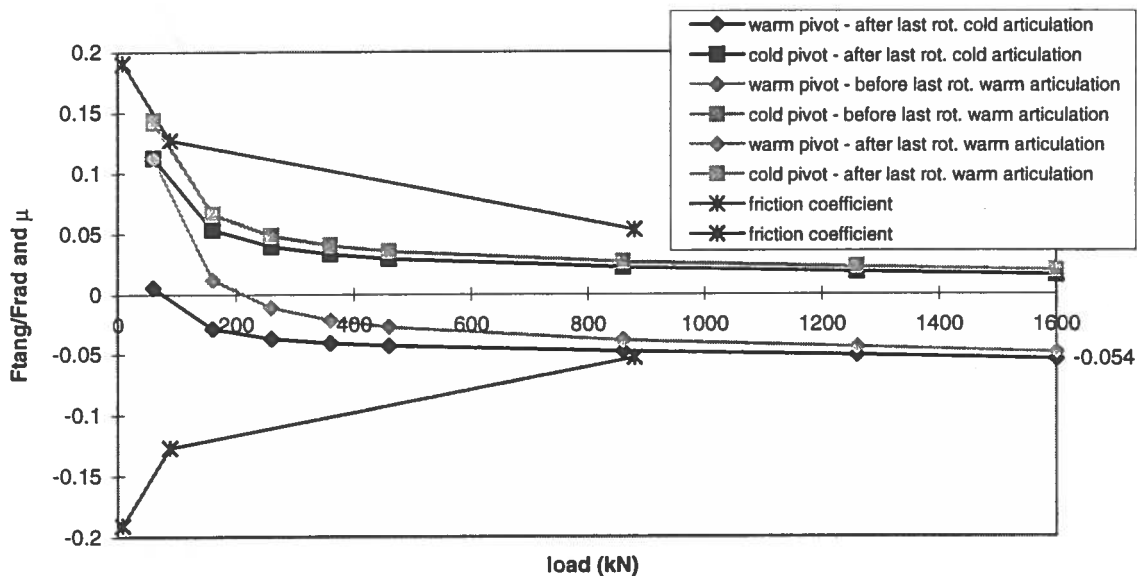


**Figure 6: The ratio between the tangential and the normal component of the pivot reaction in both the articulations during the cooldown. For comparison the values of the static friction coefficient vs. load are also reported.**

## 9. - AMPLITUDE OF THE PIVOTS ROTATION DURING SLIDING

In this analysis we have supposed the pivot rotation to stop when the ratio between the tangential and the normal component of the reaction is  $\frac{3}{4}$  of the static friction coefficient. In

this section the validity of this assumption is checked. The rotation is studied considering the energy involved in this movement and the new results are compared with the previous ones.

In the previous static analysis the inertia forces have been neglected. In this study they are included supposing the mass of the flexible part concentrated in its ends.

Variables in the initial condition are indicated by the subscript *in*, variables in the final condition have no subscript or are indicated by  $\bar{f}$ .

The study refers to the warm pivot (i.e. the fixed one). During its rotation the position and the orientation of the cold articulation don't change:

$$\begin{aligned} y &= y_{in} \\ \zeta - \theta &= (\zeta - \theta)_{in} \end{aligned} \quad (15.)$$

From these relations and equation (1) it is:

$$s = \frac{s_{in} \cos(\zeta_{in}) + (r_{ca} + h + l)(\sin(\zeta) - \sin(\zeta_{in}))}{\cos(\zeta_{in})} \quad (16.)$$

and being  $\zeta - \zeta_{in} = \theta - \theta_{in}$  small it is:

$$s - s_{in} = [r_{wa} + h + l + s_{in} \tan(\zeta_{in})](\vartheta - \vartheta_{in}) \quad (17.)$$

Using this relation in the expression of  $C_0/N$  and  $P/N$  it is:

$$\begin{aligned} \frac{C_0}{N} &= \left( \frac{C_0}{N} \right)_{in} + [X_c(r_{wa} + h + l + s_{in} \tan(\zeta_{in})) + Y_c l](\vartheta - \vartheta_{in}) \\ \frac{P}{N} &= \left( \frac{P}{N} \right)_{in} + \left[ \frac{X_p}{l} (r_{wa} + h + l + s_{in} \tan(\zeta_{in})) + Y_p \right](\vartheta - \vartheta_{in}) \end{aligned} \quad (18.)$$

The equilibrium condition of the rigid articulation gives:

$$-P(r_{wa} + h) + \text{tg}(\phi_d) F_R r_{wa} - C_0 - I \ddot{\zeta} = 0 \quad (19.)$$

where  $I$  is the inertia momentum of the rigid articulation respect to its rotation axis and it is  $\text{tg}(\phi_d) = \mu_d$  (being  $\mu_d$  the dynamic friction coefficient).

Using the previous expressions of  $C_0/N$  and  $P/N$  the motion law becomes:

$$\frac{d^2(\vartheta - \vartheta_{in})}{dt^2} + \omega^2(\vartheta - \vartheta_{in}) = Q\omega^2 \quad (20.)$$

where:

$$\omega^2 = \frac{N}{I} \left\{ (r_{wa} + h) \left[ \frac{X_p}{l} (r_{wa} + h + l + s_{in} \text{tg}(\zeta_{in})) + Y_p \right] + X_c (r_{wa} + h + l + s_{in} \text{tg}(\zeta_{in})) + Y_c l \right\} \quad (21.)$$



$$Q = \frac{1}{N} \frac{tg(\phi_d)F_R r_{wa} - P_{in}(r_{wa} + h) - C_{0,in}}{(r_{wa} + h) \left[ \frac{X_p}{l} (r_{wa} + h + l + s_{in} tg(\zeta_{in})) + Y_p \right] + X_c (r_{wa} + h + l + s_{in} tg(\zeta_{in})) + Y_c l}$$

If  $F_R$  is supposed to be constant the solution is:

$$\vartheta - \vartheta_{in} = Q[1 - \cos(t\omega)] \quad (22.)$$

with

$$\frac{d(\vartheta - \vartheta_{in})}{dt} = Q\omega \sin(t\omega). \quad (23.)$$

The derivative is null in the initial and final condition, and it is  $t_f = \pi/\omega$ .

At the end of a rotation it is:

$$\vartheta - \vartheta_{in} = 2Q \quad (24.)$$

Therefore the amplitude of a rotation is equal to  $2Q$  and depends only on the geometry and the initial condition (because of the approximations used).

At the time  $t = \pi/2\omega$  the rotation is equal to  $Q$  and the angular acceleration is null. The equilibrium condition is therefore obtained with a friction coefficient equal to the dynamic one.

## 10. - ELASTIC DEFORMATION ENERGY OF THE SUPPORT

The elastic deformation energy due to the bending of the flexible part of the support is given by:

$$H = \int_l \frac{M^2}{2EJ} dz \quad (25.)$$

where  $M$  and  $E$  are the bending moment and the Young modulus respectively.

The energy due to the tensile force  $N$  is constant because  $N$  doesn't change during the rotation. The energy due to the shearing force is neglected.

The expression of  $H$  in case of a support made of two parts with different inertia momentum is reported in appendix C.

The elastic energy decreases because of the articulation rotation and the difference between the energy of the final and of the initial configuration should be equal to the work done by the external forces.

In case of a rotation of the warm pivot a work is done by the following forces:

- The friction force that we supposed to be constant, does the work:

$$L_a = -tg(\phi_d) F_{R'wa} (\vartheta_{fi} - \vartheta_{in}) \quad (26.)$$

- The tensile force does a work because during the rotation the end of the flexible part changes its vertical position.

In case of a deformation from the undeformed shape, this work is:  $-N(l'-l)$ , where:

$$l' = \int_l \sqrt{1 + \left(\frac{d\eta}{dz}\right)^2} dz \approx \int_l \left[1 + \frac{1}{2} \left(\frac{d\eta}{dz}\right)^2\right] dz \quad (27.)$$

$$l'-l = \frac{1}{2} \int_l \left(\frac{d\eta}{dz}\right)^2 dz.$$

$l'$  is the length of the deformed line whose projection on the  $z$  axis is  $l$ . According to the approximations done  $l'-l$  is the lifting of the end of the flexible part.

The expression of  $N(l'-l)$  is reported in appendix D.

In the case of a generic rotation of the warm pivot the work done by  $N$  is:

$$L_N = -(l'_{fi} - l)N + (l'_{in} - l)N + \frac{s_{in} + s_{fi}}{2} N (\vartheta_{fi} - \vartheta_{in}) \quad (28.)$$

Where the last part is included because during the rotation also the reference axis  $z$  moves.

## 11. - COMPARISON

The results of the last sections have been used to check the study of the support movements during the cooldown. The rotation amplitude, the elastic deformation energy and the external forces work have been computed in case of a rotation of the warm pivot starting from a configuration chosen at random among those at the sliding limit. The data about energy and work are reported in the first row of table 4.

In order to improve the comparison two other configurations have been considered in which the equilibrium is supposed to be reached after a rotation 20% longer or shorter than the calculated one.

Condition	$\zeta_{in}$	$\zeta_{fi}$	$\Delta s$	$\Delta H$	$L_a$	$L_N$	$\Delta H - L_{Tot}$
computed rotation	0.00970	0.00935	-0.323	-184.20	-172.88	-11.31	0
20% greater	0.00970	0.00928	-0.387	-215.40	-207.45	-13.86	5.9
20% smaller	0.00970	0.00942	-0.258	-151.12	-138.31	-8.85	-4.0

**Table 4: Comparison between the deformation energy change and the work of the external forces in case of a rotation computed in the study of the support during the cooldown.**

The results are:

- According to the rotation amplitude study, the minimum friction coefficient necessary to have equilibrium in the final configuration is  $\text{tg}\phi = 0.1119$ . The value used in the static analysis was  $\mu_{\text{min}} = 3/4 \mu_s = 0.1125$ .
- The elastic energy variation and the work of the external forces match very well in case of the computed rotation. They don't match in case of the other rotations and the sign of the difference gives another confirmation to the study of the support movements.

## 12. - CONCLUSIONS

The analytical model developed in this study is an attempt to take into account the main physical parameters involved in the behaviour of the support during the magnet cooldown and energization. The results of the previous comparison show its consistency and the validity of the approximation done using a reduced friction coefficient to find the new equilibrium condition after each rotation.

The real behaviour of the supports will depend on many more parameters and only adequate tests on a prototype under working condition can validate this solution and the low friction material adopted. But we think that this model can be useful in the research of a good candidate for the sliding surface, and for this reason we suggest the adoption of a material with an higher friction coefficient under load than Teflon filled compounds.

## REFERENCES

- [1] "Glycodur®" SKF Catalog (1985).

## APPENDIX A: FORCE AND MOMENT APPLIED TO THE WARM END OF THE FLEXIBLE PART.

The force and the moment applied to the warm end of the flexible part of the support ( $z = 0$ ), are here reported as function of the displacement ( $s$ ) and the rotation ( $\theta$ ) of the cold end ( $z = l$ ).

$$\frac{P}{N} = -\frac{a_2}{D} \left\{ \frac{a_1 + a_2}{2a_2} \sinh(\sigma) + \frac{a_1 - a_2}{2a_2} \sinh(\delta) \right\} s + \frac{1}{D} \left\{ \frac{a_1 + a_2}{2a_2} \cosh(\sigma) - \frac{a_1 - a_2}{2a_2} \cosh(\delta) - 1 \right\} \theta$$

$$\frac{C_0}{N} = \frac{1}{D} \left\{ 1 - \frac{a_1 + a_2}{2a_1} \cosh(\sigma) - \frac{a_1 - a_2}{2a_1} \cosh(\delta) \right\} s + \frac{1}{D} \left\{ \frac{a_1 + a_2}{2a_1 a_2} \sinh(\sigma) - \frac{a_1 - a_2}{2a_1 a_2} \sinh(\delta) - (l_1 + l_2) \right\} \theta$$

Where:

$$a_i^2 = \frac{N}{EJ_i} \quad (i = 1, 2)$$

$$\sigma = a_1 l_1 + a_2 l_2$$

$$\delta = a_1 l_1 - a_2 l_2$$

$$D = \left\{ 1 - \frac{a_1 + a_2}{2a_1} \cosh(\sigma) - \frac{a_1 - a_2}{2a_1} \cosh(\delta) \right\} \left\{ \frac{a_1 + a_2}{2a_2} \cosh(\sigma) - \frac{a_1 - a_2}{2a_2} \cosh(\delta) - 1 \right\} \\ + \left\{ \frac{a_1 + a_2}{2a_2} \sinh(\sigma) + \frac{a_1 - a_2}{2a_2} \sinh(\delta) \right\} \left\{ \frac{a_1 + a_2}{2a_1} \sinh(\sigma) - \frac{a_1 - a_2}{2a_1} \sinh(\delta) - a_2 (l_1 + l_2) \right\}$$

## APPENDIX B: REACTION ON THE CONTACT SURFACE OF THE WARM PIVOT

The reaction is supposed to be symmetrically distributed over an arc whose amplitude is  $2\Delta\theta$ , with the pressure following the rule:

$$p(\theta) = p_0 \left( 1 - \frac{\theta^2}{\Delta\theta^2} \right) \quad -\Delta\theta < \theta < \Delta\theta$$

This distribution gives a radial component:

$$F_R = 2br_p \int_0^{\Delta\theta} p_0 \left( 1 - \frac{\theta^2}{\Delta\theta^2} \right) \cos(\theta) d\theta = 4br_p \frac{p_0}{\Delta\theta^2} (\sin(\Delta\theta) - \Delta\theta \cos(\Delta\theta))$$

and a tangential component due to the friction:

$$F_T = 2br_p \mu \int_0^{\Delta\theta} p_0 \left( 1 - \frac{\theta^2}{\Delta\theta^2} \right) \cos(\theta) d\theta = 4br_p \mu \frac{p_0}{\Delta\theta^2} (\sin(\Delta\theta) - \Delta\theta \cos(\Delta\theta))$$

where  $b$  is the length of the contact surface,  $\mu$  is the friction coefficient ( $\mu < \mu_s$ ), and  $r_p$  is the pivot radius.

The couple due to this distribution is:

$$C_d = 2br_p^2 \mu \int_0^{\Delta\theta} p_0 \left( 1 - \frac{\theta^2}{\Delta\theta^2} \right) d\theta = \mu \frac{4}{3} br_p^2 p_0 \Delta\theta$$

The ratio between the couple and the tangential force results:

$$\frac{C_d}{F_T} = \frac{1}{3} r_p \frac{\Delta\theta^3}{\sin(\Delta\theta) - \Delta\theta \cos(\Delta\theta)}$$

This is equivalent to a reaction in a point whose distance from the centre is:

$$r_d = r_p \frac{1}{3} \frac{\Delta\theta^3}{\sin(\Delta\theta) - \Delta\theta \cos(\Delta\theta)}$$

In the following table the ratio  $r_d/r_p$  is reported in three conditions.

$\Delta\theta$	$r_d/r_p$
$\pi/2$	1.29
$\pi/4$	1.06
$\rightarrow 0$	$\rightarrow 1$

**Table 5: The ratio  $r_d/r_p$  vs. the amplitude of the arc where reaction is applied**

Therefore if the distribution is supposed to be symmetric and the contact surface is supposed to be limited, the behaviour is almost equivalent to the one due to a reaction in a single point.

### APPENDIX C: ELASTIC ENERGY OF A SUPPORT MADE OF TWO PARTS.

The elastic energy of a support made of two parts with different inertia momentum is:

$$\begin{aligned}
\int \frac{M^2}{2EI} dz &= \frac{C_0^2}{2N} \frac{a_1}{2} [\sinh(a_1 l_1) \cosh(a_1 l_1) + a_1 l_1] \\
&+ \frac{C_0^2}{2N} \left\{ \frac{(a_1 + a_2)^2}{8a_2} [\sinh(\sigma) \cosh(\sigma) - \sinh(a_1 l_1) \cosh(a_1 l_1) + a_2 l_2] \right\} \\
&+ \frac{C_0^2}{2N} \left\{ \frac{(a_1 - a_2)^2}{8a_2} [-\sinh(\delta) \cosh(\delta) + \sinh(a_1 l_1) \cosh(a_1 l_1) + a_2 l_2] - \frac{a_1^2 - a_2^2}{8a_2} [\sinh(2a_2 l_2) + 2a_2 l_2 \cosh(2a_1 l_1)] \right\} \\
&+ \frac{P^2}{2N} \frac{1}{2a_1} [\sinh(a_1 l_1) \cosh(a_1 l_1) - a_1 l_1] \\
&+ \frac{P^2}{2N} \left\{ \frac{(a_1 + a_2)^2}{8a_2 a_1^2} [\sinh(\sigma) \cosh(\sigma) - \sinh(a_1 l_1) \cosh(a_1 l_1) - a_2 l_2] \right\} \\
&+ \frac{P^2}{2N} \left\{ \frac{(a_1 - a_2)^2}{8a_2 a_1^2} [-\sinh(\delta) \cosh(\delta) + \sinh(a_1 l_1) \cosh(a_1 l_1) - a_2 l_2] + \frac{a_1^2 - a_2^2}{8a_2 a_1^2} [\sinh(2a_2 l_2) - 2a_2 l_2 \cosh(2a_1 l_1)] \right\} \\
&- \frac{PC_0}{2N} [\cosh^2(a_1 l_1) - 1] \\
&- \frac{PC_0}{2N} \left\{ \frac{(a_1 + a_2)^2}{4a_1 a_2} [\cosh^2(\sigma) - \cosh^2(a_1 l_1)] - \frac{(a_1 - a_2)^2}{4a_1 a_2} [\cosh^2(\delta) - \cosh^2(a_1 l_1)] - \frac{a_1^2 - a_2^2}{4a_1 a_2} [\sinh(2a_1 l_1) 2a_2 l_2] \right\}
\end{aligned}$$

### APPENDIX D: THE WORK DONE BY THE TENSILE FORCE STARTING FROM THE UNDEFORMED SHAPE.

In case of a deformation starting from the undeformed shape the work done by the tensile force is:

$$\begin{aligned}
N(l'-l) &= \frac{C_0^2 a_1}{2N} \left[ \frac{a_1}{2} [\sinh(a_1 l_1) \cosh(a_1 l_1) - a_1 l_1] \right. \\
&+ \frac{C_0^2}{2N} \left\{ \frac{(a_1 + a_2)^2}{8a_2} [\sinh(\sigma) \cosh(\sigma) - \sinh(a_1 l_1) \cosh(a_1 l_1) - a_2 l_2] \right\} \\
&+ \frac{C_0^2}{2N} \left\{ \frac{(a_1 - a_2)^2}{8a_2} [-\sinh(\delta) \cosh(\delta) + \sinh(a_1 l_1) \cosh(a_1 l_1) - a_2 l_2] \right\} \\
&- \frac{C_0^2}{2N} \frac{(a_1^2 - a_2^2)}{8a_2} [\sinh(2a_2 l_2) - 2a_2 l_2 \cosh(2a_1 l_1)] \\
&+ \frac{P^2}{2N} \frac{1}{2a_1} [\sinh(a_1 l_1) \cosh(a_1 l_1) + 3a_1 l_1 - 4 \sinh(a_1 l_1)] \\
&+ \frac{P^2}{2N} \left\{ \frac{(a_1 + a_2)^2}{8a_2 a_1^2} [\sinh(\sigma) \cosh(\sigma) - \sinh(a_1 l_1) \cosh(a_1 l_1) + a_2 l_2] \right\} \\
&+ \frac{P^2}{2N} \left\{ \frac{(a_1 - a_2)^2}{8a_2 a_1^2} [-\sinh(\delta) \cosh(\delta) + \sinh(a_1 l_1) \cosh(a_1 l_1) + a_2 l_2] \right\} \\
&+ \frac{P^2}{2N} \left\{ + \frac{a_1^2 - a_2^2}{8a_2 a_1^2} [\sinh(2a_2 l_2) + 2a_2 l_2 \cosh(2a_1 l_1)] + l_2 \right\} \\
&- \frac{P^2}{2N} \left\{ \frac{(a_1 + a_2)}{a_2 a_1} [\sinh(\sigma) - \sinh(a_1 l_1)] - \frac{(a_1 - a_2)}{a_2 a_1} [-\sinh(\delta) + \sinh(a_1 l_1)] \right\} \\
&- \frac{PC_0}{2N} [\cosh^2(a_1 l_1) - 2 \cosh(a_1 l_1) + 1] \\
&- \frac{PC_0}{2N} \left\{ \frac{(a_1 + a_2)^2}{4a_1 a_2} [\cosh^2(\sigma) - \cosh^2(a_1 l_1)] - \frac{(a_1 - a_2)^2}{4a_1 a_2} [\cosh^2(\delta) - \cosh^2(a_1 l_1)] + \frac{a_1^2 - a_2^2}{4a_1 a_2} [\sinh(2a_1 l_1) 2a_2 l_2] \right\} \\
&- \frac{PC_0}{2N} \left\{ - \frac{(a_1 + a_2)}{a_2} [\cosh(\sigma) - \cosh(a_1 l_1)] + \frac{(a_1 - a_2)}{a_2} [\cosh(\delta) - \cosh(a_1 l_1)] \right\}
\end{aligned}$$